Monitoring of Land Deformation Using Terra SAR-X Data around Active Fault in the Metro Manila, the Philippines

Tomonori DEGUCHI, Yoshihiro KINUGASA and Katsumi KURITA, Japan

Key words: Philippines, creep deformation, ENVISAT, TerraSAR-X, DInSAR, InSAR time series analysis

SUMMARY

The Republic of the Philippines lies across the boundary between the Eurasian plate and the Philippine Sea plate, an area ridden with active faults and frequent earthquakes. The Valley fault, running from north to south along the eastern edge of the Manila metropolitan, is a right-lateral active fault with two to four activities recorded over the past 1400 years; the estimated recurrence cycle translates to 200 to 400 years. Creep deformation along the southern part of the fault has produced some cracks running in a north-south or northeast-southwest direction. As a result, roads and ground structures near the fault exhibit vertical displacements. In this study we measured land deformations around the Valley fault along the eastern edge of the Manila metropolitan area, by means of InSAR time series analysis using ENVISAT data and DInSAR based on TerraSAR-X data.

According to our InSAR time series analysis using ENVISAT data, several phase anomalies were detected in the Manila. Most of them could be found a strong correlation with the vertical movements due to the change of groundwater levels, the deformation at each location progresses monotonically. The maximum average deformation velocity was measured 91 mm a year. Meanwhile, some of the land deformations are independent of the groundwater levels in the surrounding of the Valley fault. The difference in measurement times may partially explain this discrepancy, but we cannot deny the possibility that it resulted from creep deformation around the Valley fault, as the spatial geometry of the surface deformation runs in parallel with the fault and sites in the eastern part of the Valley fault stopped subsiding and began moving upward in around 2007.

Though the availability of the TerraSAR-X data is limited to acquisitions in and after 2008 and there are only three acquisitions over the target area on July 8, 2008, January 29, 2009, and March 27, 2010, the DInSAR using TerraSAR-X data identified uplifts in the eastern part of the Valley fault. Because phase differences from DInSAR indicative of ground subsidence or atmospheric phase delays generally tend to be smooth over wide areas, thus, by detecting a sudden spatial change in phases, a site of creep deformation can be identified and this leads to determine if the phase difference around the site results from the creep deformation. In this study, we applied the first differentiation in east-west direction to the TerraSAR-X DInSAR results to detect a steep gradient of interferometric phases. As a result, a segment was detected in the direction parallel with the Valley fault. A further examination of the link between the steep gradients of phases and creep deformation of the Valley fault will require InSAR time series analysis using TerraSAR-X data, detailed field survey, ground-based measurements,

and tectonic investigation based on geophysical exploration techniques.

Monitoring of Land Deformation Using Terra SAR-X Data around Active Fault in the Metro Manila, the Philippines

Tomonori DEGUCHI, Yoshihiro KINUGASA and Katsumi KURITA, Japan

1. INTRODUCTION

In this study, we measured land deformations around the Valley fault, a fault line running from north to south on the eastern edge of the Manila metropolitan area in the Philippines. The measurements were determined by an Interferometric Synthetic Aperture Radar (InSAR) time series analysis using ENVISAT data and Differential InSAR (DInSAR) based on TerraSAR-X data. Over the seven years since its launch in 2002, ENVISAT has collected a vast archive of data. TerraSAR-X has an extremely short wavelength (about 3.1 cm) compared to the SAR sensors on other satellites so far launched, and this property confers a high sensitivity to land deformation. With its very high ground spatial resolution of about 3 m, TerraSAR-X is expected to yield data vital for a detailed mapping of the deformation. In this study, we measured temporal changes in land surface deformation around the Valley fault based on an InSAR time series analysis using ENVISAT data. We also attempted to use the high wavelength sensitivity and spatial resolution of TerraSAR-X to depict the precise distribution of deformation along the Valley fault and extract information instrumental to disaster management and the prediction of earthquake disaster damage.

2. STUDY AREA AND MOTIVATION

The Republic of the Philippines lies across the boundary between the Eurasian plate and the Philippine Sea plate, an area ridden with active faults and frequent earthquakes. The Valley fault, running from north to south along the eastern edge of Manila (Figure 1 (a)), the Philippine capital, is a dextral strike-slip fault with two to four activities recorded over the past 1,400 years; the estimated recurrence cycle translates to 200 to 400 years. Creep deformation along the southern part of the fault has produced stepped-V-shaped cracking running from north to south, or, more precisely, from north-northeast to south-southwest. As a result, roads and ground structures above the fault exhibit vertical displacements. Figure 1 (b) is a shaded map generated from SRTM3 data provided for free by the Jet Propulsion Laboratory (JPL). The map clearly shows the land form along the fault at lower elevations on the eastern part. According to recent studies, the last activity of the fault took place on August 19, 1658. In consideration of the estimated recurrence cycle, the region now faces a high risk of a devastating earthquake with a magnitude of 7 or higher.

The Manila metropolitan area is the nation's center of politics, economy, and culture. Over the last several decades it has rapidly grown into an overcrowded mega city with an economically active population of at least 10 million. Yet the development of social and urban infrastructures of Manila have not kept pace with the city's population growth. This leaves the city vulnerable to natural disasters like an earthquake, tsunami and typhoon. Should a large-scale earthquake strike in Manila, the damage could be tremendous. Alert to the risks, the government of the Philippines has set disaster management as a top priority in the Mid-Term Philippine Development Plan (MTPDP) and pledges a commitment to strengthening its disaster-management systems towards a goal of zero damage from disasters. The government therefore needs to quickly establish a system for monitoring changes in active faults in the region, as there have been no actual long-term observations of land deformation around the Valley fault as of today. Researchers from the Philippine Institute of Volcanology and Seismology (PHIVOLCS) are engaged in their own studies concerning GPS-based land deformation observation, but time and cost constraints have limited the measurement frequency of their observations and the planar coverage of their measurement points. Some researchers hope to use measuring techniques from a satellite to create a monitoring system capable of efficiently capturing changes around the Valley fault. In this study, we measured land deformations around the Valley fault by means of InSAR time series analysis using ENVISAT data and DInSAR based on TerraSAR-X data.

3. METHODOLOGY

DInSAR is a method for measuring land surface motions by analyzing phase differences on two SAR images taken at two different times. The phase difference calculated from a pair of DInSAR data is described as $\Delta\Phi$ in Equation (1). $\Delta\Phi$ is an unwrapped phase,

$$\Delta\Phi = \Delta\phi - \Delta\phi_{orbit} - \Delta\phi_{H} = \Delta\phi_{def} + \Delta\phi_{atm} + \Delta\phi_{noise} + \Delta\phi_{\Delta h} \tag{1}$$

where $\Delta\phi$ is the phase difference of the initial interferometric images, $\Delta\phi_{def}$ is the phase difference corresponding to the displacement of land surface, $\Delta\phi_{orbit}$ is the orbit fringe, $\Delta\phi_{topo}$ is the topographical fringe, $\Delta\phi_{atm}$ is the atmospheric phase delay component, and $\Delta\phi_{noise}$ is the noise component. $\Delta\phi_{\Delta h}$, the phase term due to elevation errors in the DEM data, can be expressed as follows:

$$\Delta\phi_{\Delta h} = \frac{4\pi B_{perp}}{\lambda\rho\sin\alpha}\Delta h \tag{2}$$

where B_{perp} is the vertical component of the orbit distance between two observations, Δh is the elevation error, λ is the wavelength, ρ is the slant range length, and α is the incidence angle.
The time wavelength of $\Delta\phi_{def}$ should be generally longer than a recurrence period of the satellite, except in the event of accidental land movements caused by volcanic eruptions, large-scale earthquakes, and the like. The time wavelengths of $\Delta\phi_{atm}$ and $\Delta\phi_{noise}$, on the other hand, are shorter than a recurrence period and frequencies of their occurrence are irregular. This being the case, $\Delta\Phi$ can be described as the following equation (3), where $\Delta\phi_{atm}$ and $\Delta\phi_{noise}$ are collectively expressed as ε.

$$\Delta\Phi = \Delta\phi_{def} + \varepsilon + \frac{4\pi B_{perp}}{\lambda\rho\sin\alpha}\Delta h \tag{3}$$

Consider a case where M pairs of interferograms are derived from N+1 scenes of SAR imagery over a single area. Suppose that the land deformation from the first observation (0th recurrence) is an unknown vector, t_n(n=1…N), and that the interferogram of the m-th pair (m=1…M) is obtained from the SAR images on the i-th and j-th recurrence (i=1…N-1, j=2…N, j>i). The variable $\Delta\Phi_m$, the phase difference composing the interferogram of the m-th pair, can be expressed Equation (4):

$$\Delta\Phi_m = t_j - t_i + \varepsilon + \frac{4\pi B_{perp}}{\lambda\rho\sin\alpha}\Delta h \tag{4}$$

Assuming, as a requisite condition, that the time wavelength of each noise component is shorter than a recurrence period and changes irregularly, and assuming also that ε follows the Gaussian distribution, the values of the unknown vector t_n and Δh will be such that minimize F in Equation (5) below.

$$F = \sum_{m=1}^{M}\left\{\Delta\Phi_m - \left(t_j - t_i\right) - \frac{4\pi B_{perp}}{\lambda\rho\sin\alpha}\Delta h\right\}^2 \tag{5}$$

A smoothness constraint is added to Equation (5) to hypothesize that the time wavelength of land deformation is sufficiently longer than the satellite's recurrence period. Specifically, it is expressed as Equation (6), representing the second order difference for t_n.

$$R = \sum_{n=1}^{N}\left(t_n - 2t_{n-1} + t_{n-2}\right)^2 \tag{6}$$

By rendering the phase difference of each interferogram, $\Delta\Phi_m$, as input data, the optimal solutions to t_n and Δh, the variables used to provide the minimum value of S, where S is the linear sum of F and R, can be estimated based on the least squares method.

$$S = \sum_{m=1}^{M} w\left\{\Delta\Phi_m - \left(t_l - t_k\right) - \frac{4\pi B_{perp}}{\lambda\rho\sin\alpha}\Delta h\right\}^2 + \mu^2 \sum_{n=1}^{N}\left(t_n - 2t_{n-1} + t_{n-2}\right)^2 \tag{7}$$

The variable w in the first term on the right side of Equation (7) is the weighting function from Tukey's biweight. The variable μ^2 in the second term is a parameter used to control the smoothness of land deformation (smoothing parameter), and is fixed to 1.0. The t_n finally obtained is regarded as a vector representing the land deformation in the line of sight after separating the atmospheric phase components and other noise components. The value is output as a total of the long-term land deformation from the first observation.

4. DATA ANALYSIS

4.1 InSAR time series analysis by using ENVISAT data

We used 33 scenes of the ENVISAT data acquired in the IS2 mode (with VV polarization and incidence angles of 19.2 to 26.7 degrees) between January 8, 2003 and December 2, 2009. Figure 2 presents land formation after (a) approximately 3 years, (b) 5 years, and (c) 7 years from the first observation day (January 8, 2003.) The figure visually depicts the increase in the number of fringes and the extent to which the deformation has expanded over time.

Figure 3 compares the land deformation and the change in the groundwater level for a period of about seven years. Figure 3 (b) was generated by converting into the vertical deformation using incidence angles, on the assumption that the land deformation occurred only in the vertical direction. The red and blue in the image represent subsidence and uplift, respectively. Figure 3 (c) is a groundwater level change map measured by JICA (1992). The red and blue in the figure likewise represent the decrease and increase of the ground water level, respectively. In comparing the two figures, we find a strong correlation between the vertical movements of the groundwater levels and the ground surface in the area enclosed in the black dotted line. Meanwhile, some of the land deformations are independent of the groundwater levels in the area enclosed in the orange dotted line. The difference in measurement times may partially explain this discrepancy, but we cannot deny the possibility that it resulted from creep deformation around the Valley fault, as the spatial geometry of the surface deformation runs in parallel with the fault.

InSAR time series analysis can synthesize long-term land deformations from individual DInSAR results, enabling measurement of temporal changes in surface deformation in pixels. Figure 4 (a) shows temporal changes in places where vertical motions are highly correlated. The deformation at each location progresses monotonically. The maximum of an average deformation velocity, -91 mm/year, was measured at D02. InSAR time series analysis thus proves capable of ascertaining land deformation temporal characteristics. This makes it very effective for visualizing temporal and spatial deformations over wide areas.

The images in Figure 4 (b) chronologically present areas with weak correlation in the ups and downs of groundwater levels, and areas where the detected changes are likely to be deformations around the Valley fault. It shows that the uplift phenomena in the western part of the Valley fault (D07 and D08) are monotonous, while the land movement in the eastern part (D06 and D09) reversed from subsidence to uplift in around 2006 or 2007. It would be difficult to conceive that these tendencies resulted from groundwater pumping. As described earlier, the north-to-south placement of the Valley fault suggests that the fault activity may have been responsible for the detected changes.

4.2 DInSAR by using TerraSAR-X data

There are only three acquisitions over the target area in the TerraSAR-X archive: July 8, 2008, January 29, 2009, and March 27, 2010. Using the three images, we prepared three interferometric pairs as follows.

Pair 1: July 8, 2008 – January 29, 2009 (B_{perp}=70.0 m)
Pair 2: July 8, 2008 – March 27, 2010 (B_{perp}=71.2 m)
Pair 3: January 29, 2009 – March 27, 2010 (B_{perp}=0.8 m)

Interferometric images of three combinations are provided in Figure 5. The roughly 3 cm waveband, the X band for TerraSAR-X, is the shortest of all of the wavelengths used by SAR instruments in operation today. A short wavelength is highly sensitive to deformation, but coherence tends to become low because of a weakness to noise. Pair 2 in Figure 5 shows excellent coherence maintained over an observation period of as long as about 19 months, but only in urban areas with artificial structures. In the vegetated southern part, no interferometric phases appeared.

The interferometric images given in Figure 5 include atmospheric phase delay in addition to ground subsidence due to groundwater pumping and land deformation around the Valley fault. Deguchi (2009) simulated that the annual cyclic and the irregular change due to the atmospheric phase delay were about 6.0 and 2.5 cm respectively. This meant that an atmospheric phase delay appeared in the TerraSAR-X imagery as a fringe worth one cycle or more, making it difficult to discriminate the phase delay from actual surface deformation. The InSAR time series analysis, on the other hand, effectively separates surface deformations from atmospheric phase delays. With only three scenes used in this study, this analysis is still difficult to apply to the TerraSAR-X data. With 10 or more scenes, we can expect to separate the atmospheric phase delay using InSAR time series analysis and measure the long-term surface deformation accurately.

5. DISCUSSION

Figure 6 is an enlarged view of phase changes around the Valley fault detected by TerraSAR-X. The following phase changes are detected.

(A) Uplift of the west side of the fault in the northern part of the Valley fault
(B) Subsidence of the east side of the fault in the northern part of the Valley fault
(C) Uplift of the east side of the fault in the southern part of the Valley fault

The InSAR time series analysis performed above measured a reversal from subsidence to uplift along the eastern part of the fault in around 2007. Phase change (C) agrees with this result. It is concluded that phase change (C) is likely to result not from atmospheric phase delays, but from the actual surface deformations captured.

A closer examination of Figure 6 reveals a sudden change in interferometric phases in the west-east direction (see the white dotted line) out of the phase changes around the Valley fault. Phase differences indicative of ground subsidence or atmospheric phase delays generally tend to be mild over wide areas. Thus, by detecting a sudden spatial change in phases, a site of creep deformation can be identified and this leads to determine if the phase difference around the site results from the creep deformation. To this end, the first differentiation was applied to TerraSAR-X Pair 2 in the west-east direction for edge detection on the interferometric images. The red dotted line in Figure 7 indicates the position of the Valley fault provided in existing documents. The white line shows a steep gradient of phases detected through the first differentiation. These two lines can be determined as roughly parallel, but disagree slightly in the two areas circled in the yellow and light-blue dotted lines. The former is slightly offset toward the east from the known position of the fault. The latter is a steep gradient of phases detected at a site where the existing documents make no mention of a fault. The following three ideas are possible explanations for this disagreement.

(1) A new deformation phenomenon has started at a site without known faults.
(2) The location of deformation has moved.
(3) Faults are dispersed.

(3) is considered to be the most likely explanation at the present. If faults are dispersed, any attempt to recognize deformation by relying on topographical information and visual observation above the ground would be difficult and may have led to the disagreement. If the combination of DInSAR and edge detection based on first differentiation allowed us to detect deformation in places where no information is available, it would mean we managed to extract information instrumental to disaster management and the prediction of earthquake damage. Furthermore, edge detection of interferometric phases requires a high spatial resolution and a high phase sensitivity. This analysis method is expected to make effective use of the features of TerraSAR-X in the future. First, however, we need to confirm whether the phase changes detected in this study were caused by creep deformation. On this account, it is necessary to carry out detailed ground truth, ground-based surveys and geophysical exploration techniques.

6. CONCLUSION AND FUTURE WORK

In this study we measured land deformations around the Valley fault, a fault line running from north to south along the eastern edge of the Manila metropolitan area in the Philippines, by means of an InSAR time series analysis using ENVISAT data and DInSAR based on TerraSAR-X data. According to our InSAR time series analysis using ENVISAT data, sites in the eastern part of the Valley fault stopped subsiding and began moving upward in around 2007. Though the availability of the TerraSAR-X data is limited to acquisitions in and after 2008, the DInSAR using TerraSAR-X data identified uplifts in the eastern part of the Valley fault. We applied the first differentiation to the TerraSAR-X DInSAR results to detect a steep gradient of interferometric phases. As a result, a segment was detected in the direction parallel with the Valley fault. A further examination of the link between the steep gradients of phases and creep deformation of the Valley fault will require detailed ground truth, ground-based surveys, and geophysical exploration techniques.

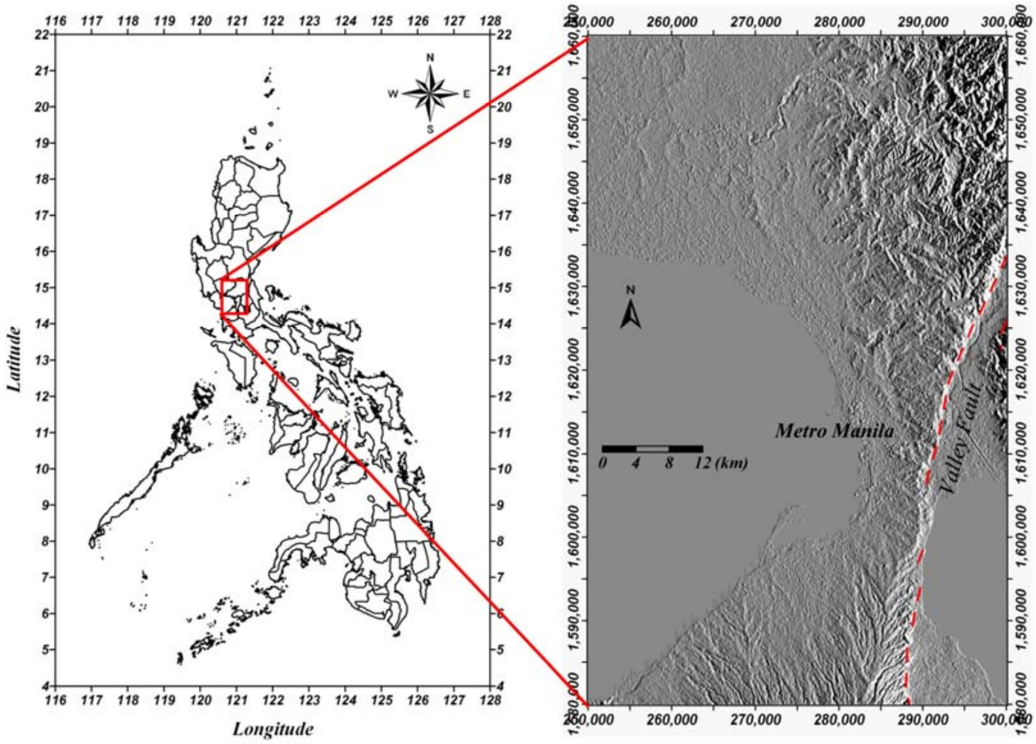

(a) Location of Study Area (b) Shaded Image generated from SRTM3

Figure 1 (a) Location of study area and (b) shaded image generated from SRTM3.

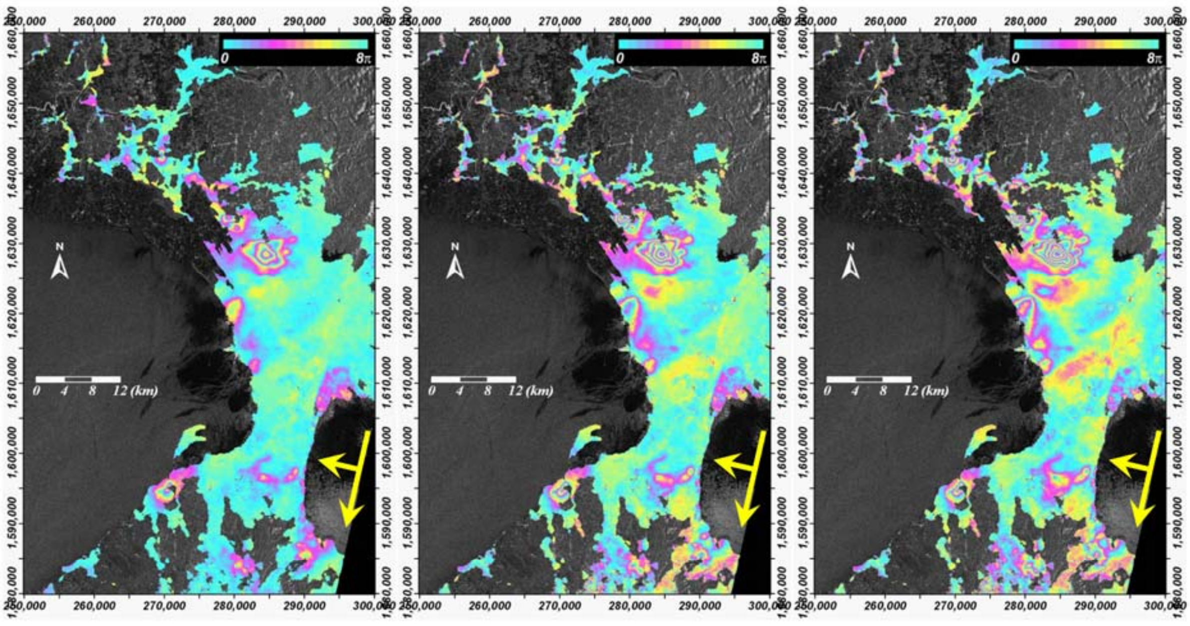

(a) 3 years
2003/01/08-2005/12/28

(b) 5 years
2003/01/08-2008/01/02

(c) 7 years
2003/01/08-2009/12/02

Figure 2 Results of InSAR time series analysis using ENVISAT data.

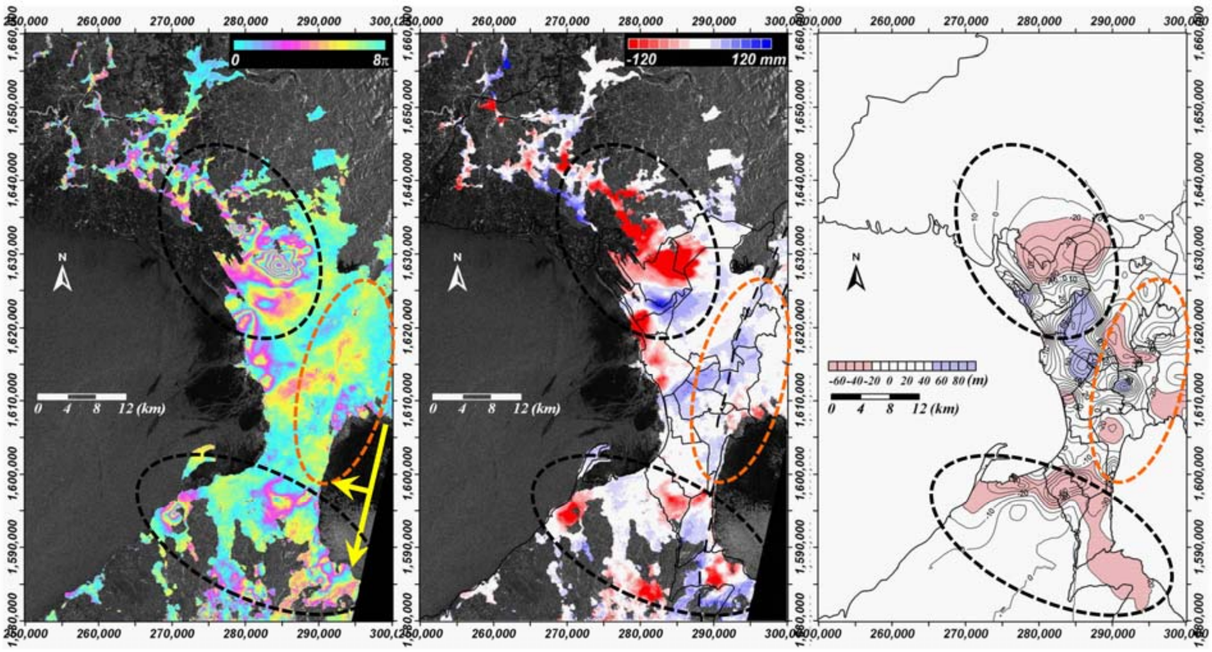

(a) Result of InSAR time series analysis
2003/01/08-2009/12/02

(b) Deformation map in the vertical direction
2003/01/08-2009/12/02

(c) Change map of groundwater level from 1981 t o1990
Japan International Cooperation Agency (1992)

Figure 3 Comparison between land deformation captured by InSAR time series analysis and the change of groundwater level.

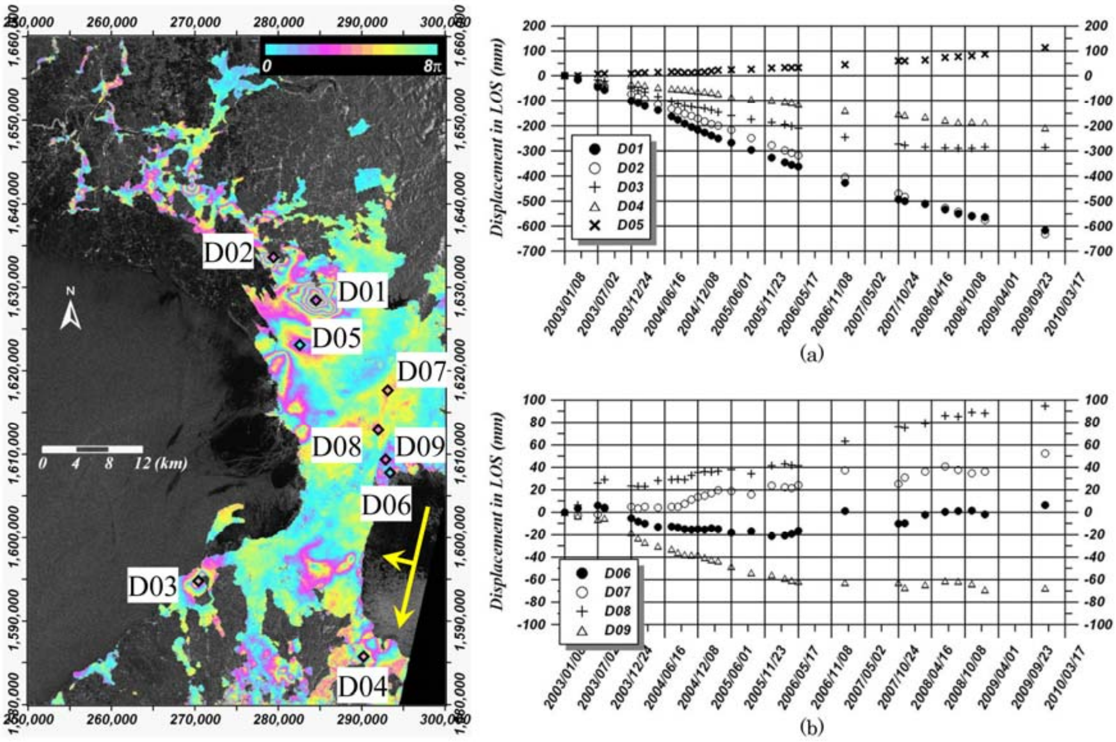

Figure 4 The profiles of temporal change of land deformation.

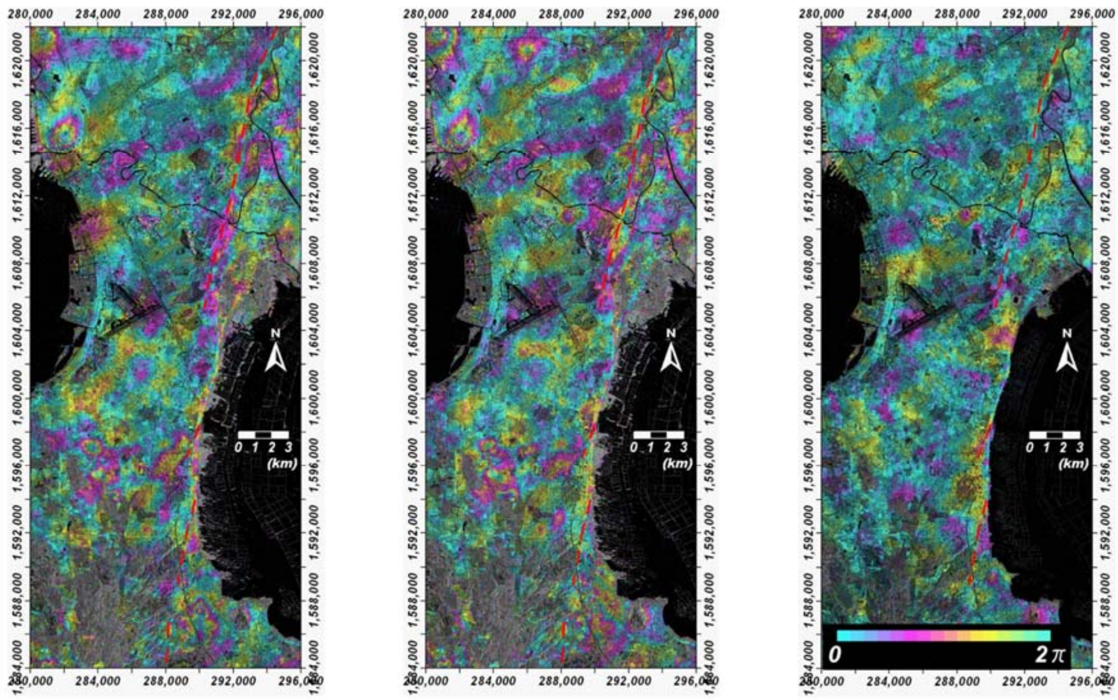

(a) Pair 1 (B_{perp}=70.0m)
2008/07/08 - 2009/12/29

(b) Pair 2 (B_{perp}=71.2m)
2008/07/08 - 2010/03/27

(c) Pair 3 (B_{perp}=0.8m)
2009/12/29 - 2010/03/27

Figure 5 DInSAR result using TerraSAR-X data.

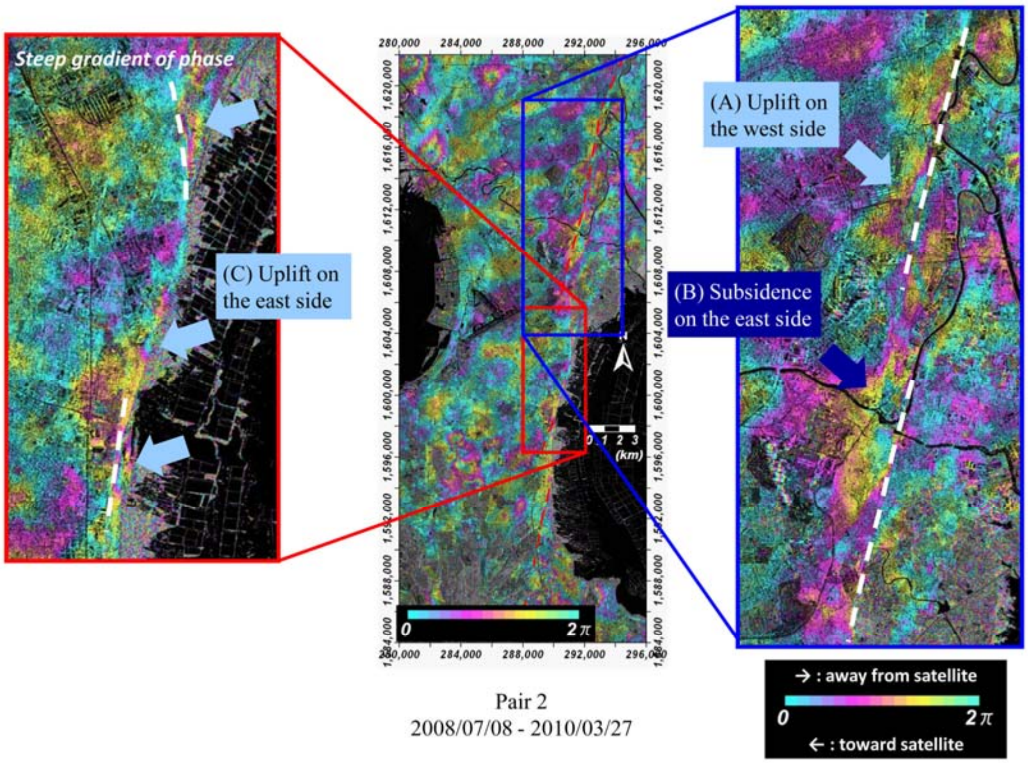

Pair 2
2008/07/08 - 2010/03/27

Figure 6 Enlarged images in the surrounding of Valley fault.

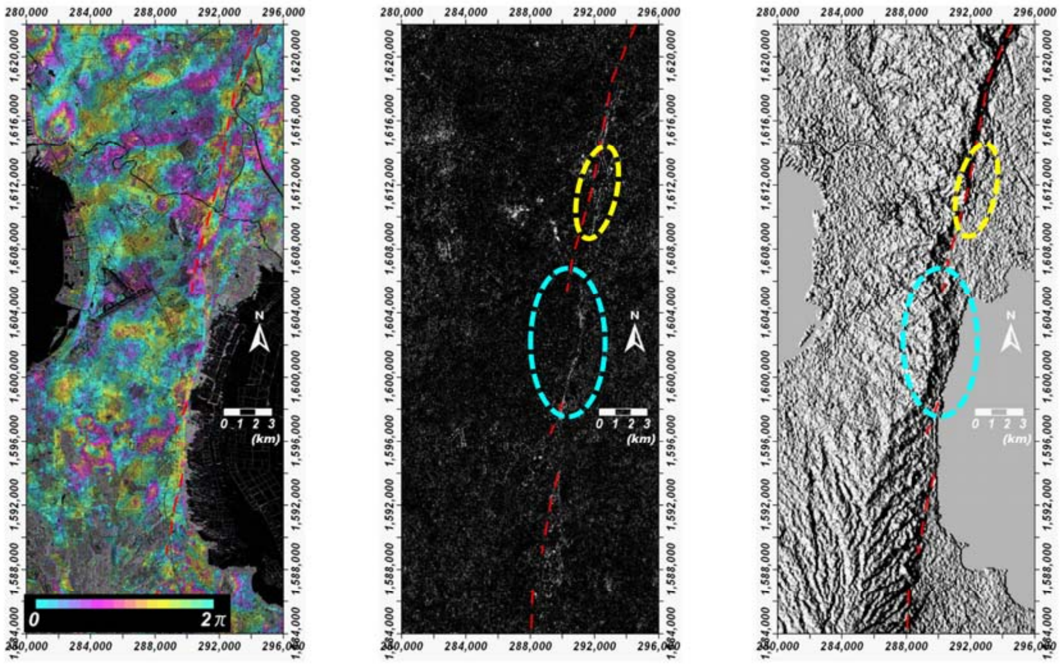

(a) Pair 2
2008/07/08 - 2010/03/27

(b) Edge Detection by the first differentiation

(c) Shaded Image of SRTM3

Figure 7 Result of edge detection using the first differentiation.

REFERENCES

Japan International Cooperation Agency : Republic of the Philippines Metropolitan Waterworks and Sewerage System, Study for the groundwater development in Metro Manila, Summary Report, Volume 1-4, 1992.

Bautista M. L. P., and Oike K. : Estimation of the magnitudes and epicenters of Philippine historical earthquakes, Tectonophysics, vol.37, No.1-2, pp.137-169, 2000.

Nelson A. R., Personius S. F., Rimando R. E., Punongbayan R. S., Tungol N., Mirabueno H., and Rasdas A. : Multiple Large Earthquakes in the Past 1500 Years on a Fault in Metropolitan Manila, the Philippines, Bulletin of Seismological Society of America, 90, 1, pp.73-85, 2000.

Japan International Cooperation Agency : Earthquake impact reduction study for Metropolitan Manila, Republic of the Philippines, Final Report, Volume 1-6, 2004.

Rolly E. R., and Petet L. K. K. : Neotectonics of the Marikina Valley fault system (MVFS) and tectonic framework of structures in northern and central Luzon, Philippines, Tectonophysics, 415, pp.17-38, 2006.

Deguchi T. : A Study on Application and Practical Use of SAR Interferometry for Ground Deformation Measurement, Ph.D. paper of the University of Tokyo, 2009.

CONTACTS

Tomonori Deguchi
Nittetsu Mining Consultants Co., Ltd.
4-2-3 NOF Shiba Building 5F, Shiba, Minato-ku, Tokyo, JAPAN
Tel. +81-3-6414-2766
Fax +81-3-6414-2772
Email: t_degu@nifty.com
Web site: http://www.nmconsults.co.jp/english/english_top.html